POWDER-IN-TUBE TAPES OF MgB_2 IN Fe-SHEATH PROCESSED BY *EX-SITU* SPARK PLASMA SINTERING

Mihail BURDUSEL[1, 2], Alina Marinela IONESCU[1], Mihai GRIGOROSCUTA[1,2], Dan BATALU[2], Monica ENCULESCU[1], Stelian POPA[1], Valentina MIHALACHE[1], Gheorghe ALDICA[1], Petre BADICA[1]

Commercial MgB_2 powder was loaded into a Fe-tube, by plastic deformation a tape of ~0.5 mm in thickness and 6.9 mm in width was obtained. Short pieces were processed by Spark Plasma Sintering (SPS) at 950, 1050 and 1150 ℃ for 3 min. The optimum sintering temperature is 1050 ℃. From magnetic/electrical measurements, the onset critical temperature and the irreversibility field at 5 K were 38.7 / 38.9 K and 6.2 / 13.5 T, respectively. The pinning-force-related parameters indicate that the dominant flux pinning mechanism is of point pinning type. Contribution of grain boundary pinning is stronger at lower temperatures.

Keywords: MgB_2, Spark Plasma Sintering, tapes, superconductivity, pinning mechanism

1. Introduction

The MgB_2 superconductor receives much attention for different applications. This is because it has a relatively high critical temperature of ~39 K. It is composed of cheap and available elements without noble metals or rare earths as in the case of technical low temperature and high temperature superconductors. MgB_2 has also low anisotropy and the coherence length is relatively long. The last feature allows use of MgB_2 as a randomly-oriented polycrystalline material making the fabrication costs of superconducting wires and tapes much lower comparative to cuprate superconductors that require a 3D epitaxial structure. It is also a light-weight superconductor valuable for portable applications.

Different methods of MgB_2 wires and tapes fabrication have been reported. We mention diffusion of Mg into B [1–3], hybrid physico-chemical vapor deposition [4–9], molten salt electroplating [10], and different variants of the powder in tube technique (PIT) [11–20]. The PIT method is the most popular; it is relatively simple and can be rapidly scaled up for large scale production. In the PIT method, a metal tube is filled in with powders and it is subject to plastic

[1] National Institute of Materials Physics, Magurele Platform, Romania, e-mail: mihaita_burdusel@yahoo.com
[2] Faculty of Materials Science and Engineering, University POLITEHNICA of Bucharest, Romania

deformation (drawing, extrusion, swaging) and annealing procedures. If raw materials are Mg and B the method to obtain the MgB_2 bulk core is named *in situ*, while if the MgB_2 compound is the raw material, the approach is considered *ex situ*. The annealing is applied at intermediate stages of mechanical deformation of the wire/tape-forming for stress relaxation [16, 17]. After deformation is completed, annealing is used to react and/or sinter the tube's powdered load [21–24]. The *in situ* method uses low temperatures of final annealing (600-800 °C), while *ex situ* one needs higher temperatures (900-1200 °C) [25]. The two approaches have advantages and disadvantages. In the *in situ* route the density and grain connectivity are poor [26-29] and limit current carrying capacity. To improve connectivity of the MgB_2 core, in the *in situ* method, different routes were tested with more or less success. We mention cold pressing, [30-33], self-propagation synthesis [34] or hot isostatic pressing [35]. On the other hand, in the *ex situ* route, high processing temperatures promote inter diffusion between metal sheath and MgB_2 [36, 37]. Under these circumstances the number of potential suitable sheath materials is limited. To overcome the problem and considering also that MgB_2 is recognized as a difficult-to-sinter material [21, 22], pressure-assisted high temperature processing methods such as hot pressing or spark plasma sintering [38, 39] and activation approaches such as ball milling [25] are of much interest. These methods can decrease sintering temperature and time for enhancement of densification, while the inter diffusion is minimized. Among them, very promising is SPS. This method is flexible allowing high heating and cooling rates and in general is viewed as a fast sintering technique [40]. It applies a uniaxial pressure on a mould-punches system loaded with the sample. Heating is realized by a current passing through the mould-punches system and the sample. The current has a pulsed component and it is often debated in literature [41] to induce useful unconventional activation effects. We have proposed that a continuous SPS variant, namely the 'spark-plasma-rolling' (SPR), would be appropriate for fabrication of MgB_2 wires/tapes [42]. To the authors' knowledge, a SPR machine is not available. To assess the feasibility of a SPS-like-approach use in the future for processing of the MgB_2 wires/tapes, in this work we applied the classic *ex situ* SPS on short pieces of PIT MgB_2 –Fe tapes. The procedure was similar to that for optimum MgB_2 bulks [43, 44] and the only varied parameter was SPS temperature. Namely, temperatures were 950, 1050 and 1150 °C. The best sample fabricated for 1050 °C was subject to complex characterization.

2. Experimental

A single core MgB_2 tape has been fabricated *by powder-in-tube* technology. The MgB_2 powder, supplied by Alpha Aesar (99.5 % purity), was loaded into a Fe tube pressed at one end. The tube had an initial outer diameter of

3 mm and the inner one of 1.8 mm. After closing the tube at the second end by pressing, it was submitted to few steps of cold plastic deformation (tube reduction was 0.1 mm) on a flat rolling machine Durston (UK). This step produced two parallel faces necessary for the subsequent pressing step. The final plastic deformation step was cold pressing under a load of 220 kN. As-pressed tape had a width of 6.9 mm, thickness of 0.5 mm and a length of ~30 mm. The part of the tape with MgB_2 core was of about 20 mm. A piece of ~15 mm cut from the tape containing the MgB_2 core was submitted to a SPS treatment. Tapes were immersed in an inert powder within a graphite mould-punches system. A FCT Systeme GmbH HP D 5 SPS furnace was used. The parameters of the SPS procedure were: heating rate 110 °C/min, dwell time 3 min, maximum pressure 96 MPa. SPS temperatures were 950, 1050 and 1150 °C. The initial vacuum in the SPS chamber was ~30 Pa. Chamber was washed with Ar for two times. These parameters were selected based on our previous optimization experiments for bulk samples [43, 44].

X-ray diffraction (XRD) patterns were taken with a Bruker AXS D8 Advance diffractometer (CuK_α radiation) on the MgB_2 core after peeling the Fe-metal sheath.

Surfaces of the peeled core and the inner face of the sheath were observed by scanning electron microscopy (Zeiss EVO50).

Magnetic measurements were performed with a VSM magnetometer (Cryogenics) on the peeled superconducting core of the SPSed tape. Sample was of (L = 2.44 mm) x (l = 1.76 mm) x (G = 0.25 mm) (L x l *x* G, L = length, l = width and G = thickness). The magnetic field was applied parallel to the sample thickness and to the direction of the uniaxial pressure used during SPS processing. The critical current density at different temperatures, J_c, was determined from the $m(H)$ experimental loops with Bean formula for a plate-like geometry [45]:

$$J_c = 20 \cdot | m\uparrow - m\downarrow | / (V \cdot l \cdot (1-(l/(3 \cdot L)))) \quad (1)$$

where m is magnetic moment in emu on ascending and descending magnetic field, V – the sample volume in cm^3, and L, l are in cm. Prior to J_c-determination, corrections of the magnetic hysteresis loops to eliminate the magnetic contribution of the impurities, and the holder were undertaken. Flux jumps were not considered and, hence, they were removed from the J_c-H curves. The irreversibility field H_{irr}^{mag} was determined for a criterion of 100 A/cm^2. The volume pinning force $F_p = J_c \cdot H$ was extracted and plotted as a function of H. The reduced pinning force $f_p = F_p / F_{p,\,max}$ is represented as a function of the reduced magnetic field $h = H / H_{irr}^{mag}$.

The resistivity as a function of temperature under a magnetic field H = 0 – 14 T was investigated on the tape's core using the four probes method in a PPMS-Quantum Design equipment. Sample size was L = 5.985 mm) x (l = 5 mm) x (G = 0.25 mm). The measuring current (2 mA) was applied in the $L \cdot l$-plane and in the

L-direction, while *H* was parallel to *G*. Electrical contacts were made with Ag-paste. The irreversibility field $H_{irr}^{electric}$ was determined for a criterion of 10 % of the superconducting transition in the resistivity curve [46].

3. Results and Discussion

3.1 Aspects of the relationship between processing, structure and microstructure

The experiment at high SPS temperature of 1150 °C was not successful. Namely, the integrity of the tape was not preserved. A strong melting of the metal sheath was observed and sample was not superconducting. The reason is reaction of Fe with B to form Fe_2B. The Fe-B phase diagram [47] shows a eutectic point at 1149 °C. This transformation is likely reflected by a strong slope change in the approximately linear displacement curve vs. temperature above 1132 °C (Fig. 1, sample SPSed at 1150 °C). We selected the SPS temperature of 1150°C because this was the optimum one established for the SPS processing of the bulk MgB_2 samples [43] and expectations were that SPS processing time is short enough to avoid the indicated reaction. We lowered the SPS temperature to 1050°C. In this case sample was superconducting, but some inter diffusion between Fe sheath and MgB_2 core was observed. Nevertheless, peeling was possible and the inner surface of the Fe sheath is relatively clean and uniform (Fig. 2 a, b). The outer surface of the MgB_2 – core peeled from the SPSed tape processed by SPS at 1050 °C was of slightly golden color and EDS indicated the presence of some Fe. Contamination of the core with Fe is reasonably low and this idea is supported by the fact that in the XRD pattern of the core, the Fe-based impurity phases cannot be clearly distinguished (Fig. 3). The major impurity phases in the core are MgO and MgB_4. Their presence suggests similar main reactions as those proposed for the SPSed bulks [43], this being also in good agreement with reported phase diagrams [48]:

$$2MgB_2 \rightarrow MgB_4 + Mg \quad (2)$$

$$2Mg + O_2 \rightarrow 2MgO \quad (3)$$

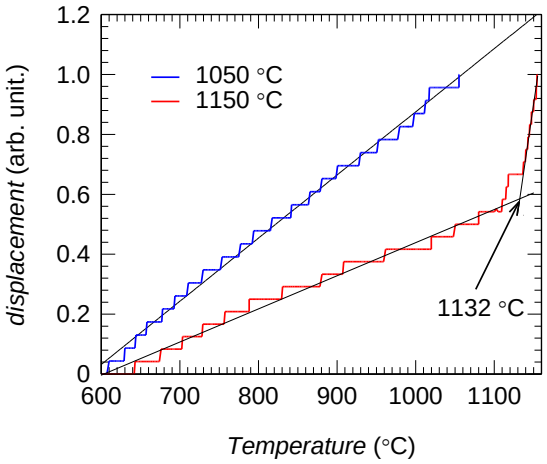

Fig. 1. Displacement curves with temperature for samples SPSed at 1050 and 1150 °C

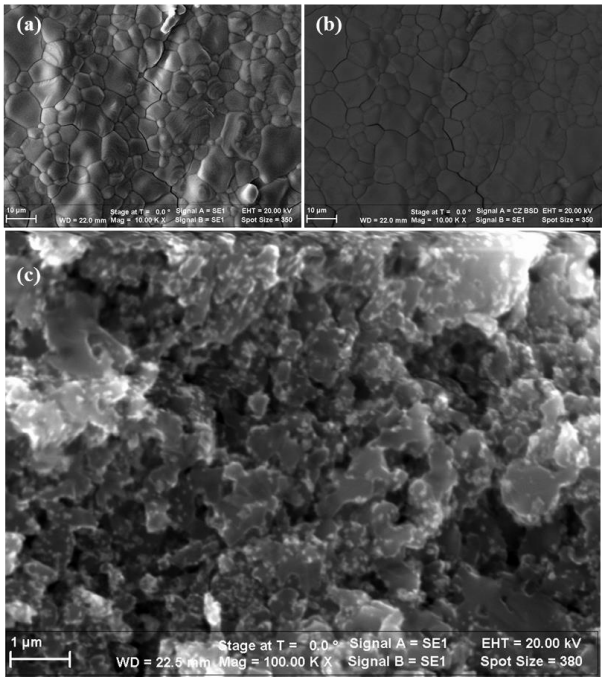

Fig. 2. SEM image of the MgB_2 core tape, (a) and (c) taken in secondary electron mode and (b) in back scattering mode.

The oxygen is the accidental one and can be from the involved materials (e.g. raw powder, Fe tube, mold system, SPS furnace) or it can be introduced in the process of loading the MgB_2 powder into the Fe-tube. Our experiments of loading the powder into the Fe tube under pure Ar atmosphere in a glove box with the oxygen purity of 0.1 ppm has shown no significant influence on the phase

content of the sintered tape. It is inferred that the most probable sources of the oxygen are the raw powder and the Fe-tube, but further investigations are necessary to confirm this speculation.

The fractured cross section of the core (Fig. 2 c) from the tape processed by SPS at 1050 °C shows the typical morphology of MgB_2 composed of submicron grains and of sintered agglomerates. The size of agglomerates is higher than 1 μm, typically being of ~5 - 10 μm. In the bulk SPSed samples at 1150 °C [43] agglomerates are larger (20 - 100 μm). A higher temperature promotes sintering and sheath-core inter diffusion. Indeed, our tape processed by SPS at a lower temperature of 950 °C has shown easy detachment of the core from the Fe sheath, but even in these conditions it was fragmented into many pieces with a powdered appearance. It was not possible to extract a relatively large piece suitable for electromagnetic measurements. We conclude that, although it diminishes inter diffusion, a SPS temperature of 950 °C is low for efficient sintering and fabrication of the tape. The optimum SPS temperature is 1050 °C. This sample was electromagnetically characterized in detail and results are presented in the next paragraphs.

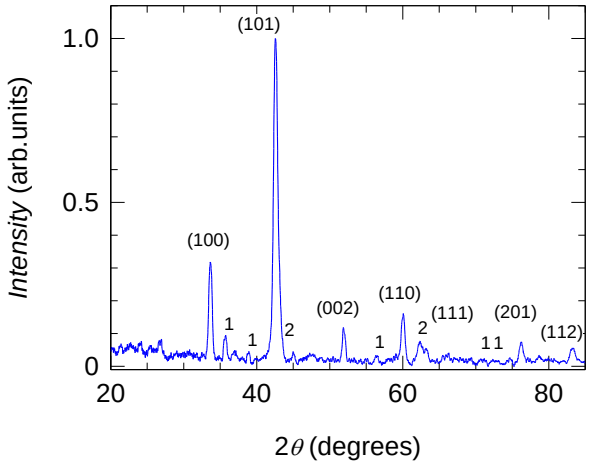

Fig. 3.X-ray diffraction patterns for MgB_2 core tape. Phases are: MgB_2 (ICDD38-1369), 1-MgB_4 (ICDD15-0299) and 2-MgO (ICDD45-0946). The (hkl) planes are indicated for the MgB_2 phase.

3.2 Superconductivity characterization of the tape processed by SPS at 1050 °C

The sample processed at 1050 °C has a *zero-field-cooling* magnetic transition in the superconducting state (Fig. 4) with an onset critical temperature of 38.7 K. Transition is sharp and magnetization is saturated below ~35 K. The shape of the $m(T)$ curve is similar to that of the bulk samples processed by SPS [43]. The curve of resistivity R vs. temperature at H = 0 T shows a critical temperature of 38.9 K (Fig. 5). The two critical temperatures, magnetic and

electrical, are in good agreement. The fact that the critical temperature from the electrical measurement is slightly higher is the consequence of the differences and specifics of each type of the measurement. The electrical one shows the most convenient percolation-current-path involving the best superconducting regions, i.e. the regions with the highest $T_c(R=0)$, while in the magnetic measurement the super current tends to close into a loop over the contour of the sample not necessarily involving only the best regions. The two measurements are also different considering that the magnetic one is performed under an external magnetic field of 100 Oe that decreases the critical temperature and the transport one is in zero-field.

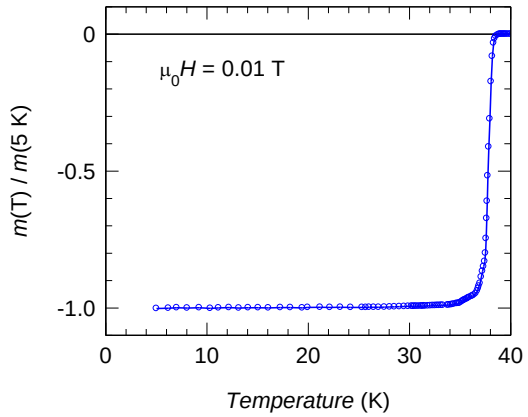

Fig. 4. Normalized magnetic moment vs. temperature for *zero-field-cooling* conditions.

The normal state behavior of the MgB_2 core is metallic (Fig. 5a), but at low temperatures it departs from a linear one. For free parameters ρ_0, A and m, a good fit of the experimental data by the least-square method (Fig. 5) is obtained with the function:

$$\rho(T) = \rho_0 + AT^m \tag{4}$$

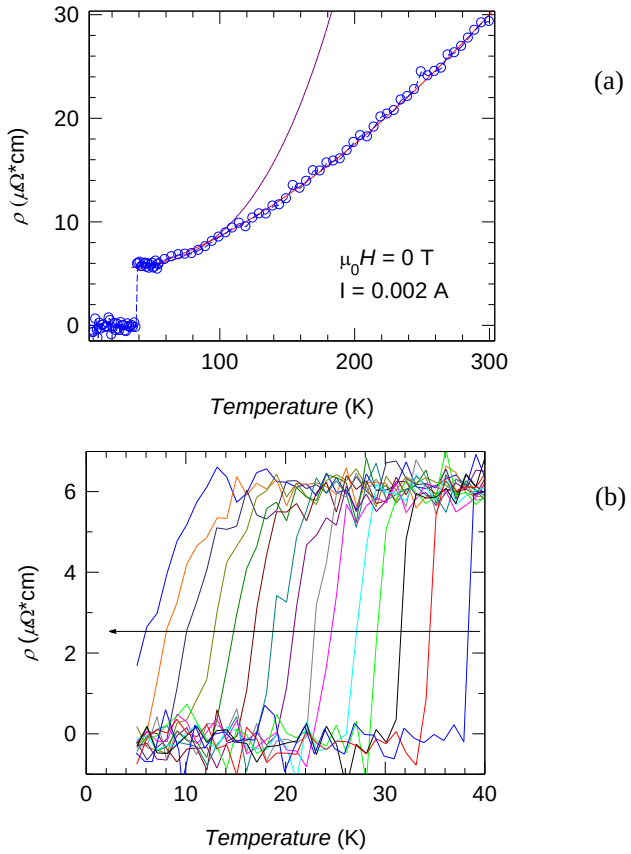

Fig. 5. The MgB_2 tape core: (a) - temperature dependence of the electrical resistivity (ρ) and power fit (see text); (b) – superconducting transitions measured in magnetic fields between 0 and 14 T (the arrow indicates the increase of the applied magnetic field).

The resulting parameters are ρ_0 = 4.5 μΩ·cm, A = 1.884 x 10^{-3} μΩ·cm·K^{-1} and m = 1.66, while the maximum deviation is 1.1 mΩ·cm and the coefficient of determination r^2 is 0.9982. The value r^2 indicates the goodness of the fit and a higher value closer to 1 is for a better fitting [49]. One observes that m > 1, but not much different from 1. At low temperatures, from theoretical considerations m = 3 [see e.g. 46 and therein refs.]. Indeed, a fit of experimental data for T = 40 - 120 K results in m = 3.29 and ρ_0 = 5.5 μΩ·cm and it generates a curve that deviates from the experimental data at a temperature of ~93 K (Fig. 5a). This temperature represents 0.1 of Debye temperature (θ_D) [46], and thus, θ_D = 930 K. The values of ρ_0 from both fits are reasonably close to each other. They are also relatively similar to the experimental value ρ^{40K} = 6 μΩ·cm of the zero-field resistivity at 40 K (40K is arbitrary taken as the onset temperature of the superconducting transition). The ratio (*RRR*) between the resistivity at room

temperature ρ^{300K} = 29.3 μΩ·cm and the one at the onset temperature ρ^{40K} is ~4.8, while their difference is $\Delta\rho$ = 23.3 μΩ·cm. In literature, the values of ρ^{40K}, ρ^{300K}, *RRR*, $\Delta\rho$ and θ_D for the phase-pure MgB_2 [46 and therein refs.] are of: ~1-50 μΩ·cm, ~10-100 μΩ·cm, ~2-20, ~7-50 μΩ·cm, and ~ 1000-1500 K [46 and therein refs.]. Our experimental values are within the values for a pure phase MgB_2. However, it was suggested that a higher ρ^{300K} and a lower RRR indicate a higher disorder in the samples. Disorder is associated with the presence of residual strain, defects and of nano-metric impurities. The residual strain, defects and nano impurities can play the role of effective pinning centers. The presence of pinning centers is desired for the enhancement of the key functional parameters, namely the critical current density, J_c, and the irreversibility field H_{irr}. Information on impurities is provided also by the temperature independent ρ_0 which is the residual impurity scattering part of the resistivity in eq. 4. There are also other aspects to be taken into consideration when analyzing the resistivity values. Impurities (MgO and MgB_4 as-detected by XRD, Fig. 3) and pores (Fig. 2) impede the supercurrent flow and the consequence is that connectivity decreases. Rowell [27] has shown that these non-superconducting regions have a high impact on resistivity curves. For a thin film of MgB_2 that is supposed to be without pores $\Delta\rho$ is small of about 7 μΩ·cm [27], while for the core of our tape it is 23.3 μΩ·cm. i.e. it is about 3.3 times higher for the core. The meaning is that the connectivity of the core in our tape is roughly 3 times lower than for the film. Hence, the corrected resistivity $\rho^{300K}_{corrected}$ or the true resistivity within the MgB_2 grains themselves is 29.3 / 3.3 = 8.8 μΩ·cm. This value is slightly lower than 13 μΩ·cm for the bulk sample obtained in ref. [46] by an in-situ route. The disorder in our MgB_2 is somehow lower. The result may look surprising considering that SPS is a technique far from equilibrium and tapes were subject to mechanical deformation at room temperature; our processing route was expected to produce a higher level of disorder. The discrepancy is related to the impossibility to compare two different technologies and to the problems encountered in precise assessment and evaluation of different contributions (e.g. from pores, grain boundaries, impurities, crystal quality of the MgB_2 grains, defects and residual strain) on the normal state resistivity.

With the increase of the external magnetic field *H*, $\rho(T)$ transition curves shift in a parallel manner to lower temperatures (Fig. 5b). The irreversibility field $H_{irr}^{electric}$ extracted from these curves is shown in Fig. 6.

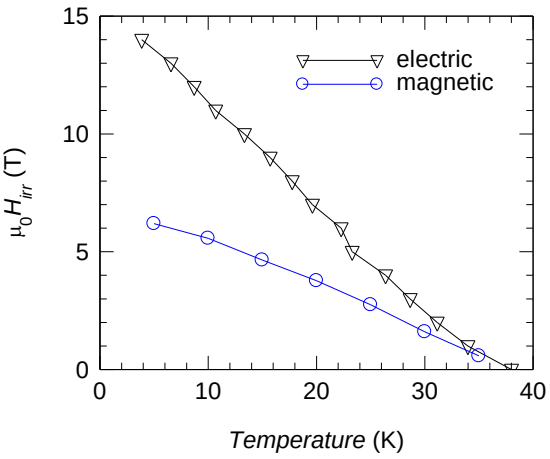

Fig. 6. The irreversibility field dependences with temperature.

The corrected magnetization loops at different temperatures are plotted in Fig. 7. Curves of $H_{irr}^{mag}(T)$, $J_c(H)$, $J_{c0}(T)$ and $J_{c0}{\cdot}H_{irr}^{mag}$ (T) extracted from the magnetization loops are presented in Figs. 6, 8-10. The product $J_{c0}{\cdot}H_{irr}^{mag}$ (T), defined as a *quality factor* is a sort of mediated pinning force or a magnetic energy and it shows the balance between the low-field and high-field properties [50]. It has no physical or practical technical meaning, but it provides extra comparative information about the samples quality. At 5 K the values of $H_{irr}^{mag}(T)$, $J_{c0}(T)$ and $J_{c0}{\cdot}H_{irr}^{mag}(T)$ are 6.19, 0.875, and 5.416, respectively. At 20 K they are 3.77, 0.576 and 2.171. We note that for the bulk sample obtained by SPS at 1150 °C, the values at 5K are 7.522, 0.814 and 6,128, and at 20 K they are 4.09, 0.54 and 2.208 [50]. Results suggest that the quality of the MgB_2 core of the tape is reasonably high when compared with the bulk sample. One can also observe that H_{irr}^{mag} is lower than $H_{irr}^{electric}$ (Fig. 6). As already addressed, this is because of the electrical and magnetic measurements specific features.

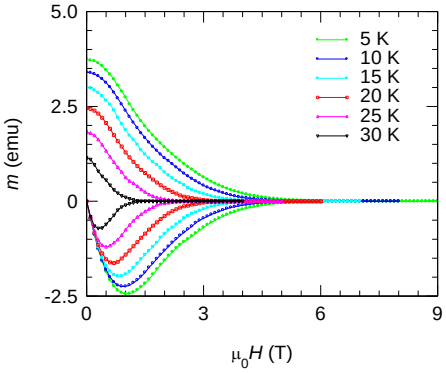

Fig. 7. Magnetization loops versus magnetic field for MgB_2 core tape at 5-30 K.

Experimental curves of reduced pinning force f_p as a function of the reduced magnetic field h (Fig. 11) were fitted with the universal scaling law $f_p = Bh^p(1-h)^q$ [51]. Scaling with the popular Kramer function $f_p = Bh^{1/2}(1-h)^2$, where $h = H / H_{c2}$ (H_{c2} is the upper critical field) produces unrealistic results [52] in the case of MgB_2. It is necessary to use the universal scaling law $f_p = Bh^p(1-h)^q$ [51]. Uncertainties in determination of H_{c2} pointed on the necessity of using H_{irr}; H_{c2} is replaced with H_{irr} [52 and therein refs.] in the universal scaling law. This has found its justification in the models based on Anderson–Kim theory where the scaling field is the irreversibility field. We also eliminated in the fit of our experimental f_p-h data, the points where $f_p \leq 0.02$ and h takes values toward 1. Another region eliminated from the fit is for $h \leq H_{\text{of the full penetration}} / H_{irr.}$ The f_p-h experimental points taken into consideration for the fit at different temperatures are presented in Fig 11. An example showing experimental points at 5 K and their fitting curve with the universal scaling function is given in Fig. 11 inset. Fitting parameters p and q give information on the dimension of the pinning manifold and pinning type [51]. The condition is that only one pinning mechanism is dominant and in such a case for the pinning on grain boundaries (GPB) in isotropic samples ($p = 0.5$, $q = 2$), the scaled pinning force reaches a peak for a reduced field $h_0 = 0.2$, while for the pinning on point (PP) like defects ($p = 1$, $q = 2$) the maximum locates at $h_0 = 0.33$. These situations are for (normal) core pinning, while for (normal) magnetic pinning ($p = 0.5$, $q = 1$) $h_0 = 0.33$ [51].

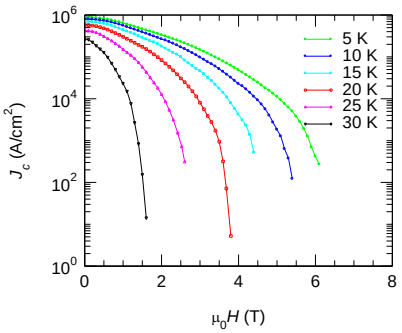

Fig. 8. Critical current density vs. magnetic field at 5- 30 K.

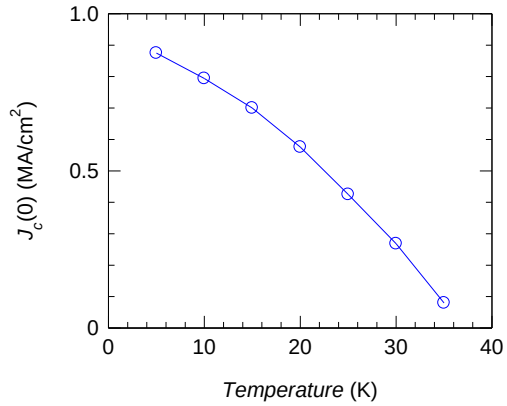

Fig. 9. Zero-field critical current density vs. temperature.

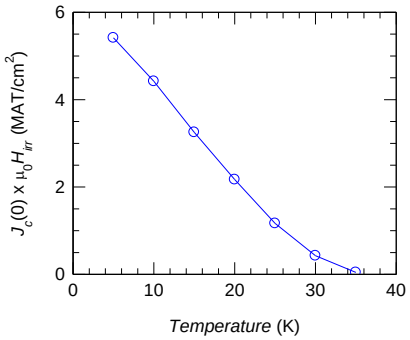

Fig. 10. The product ($J_{c0} \cdot \mu_0 H_{irr}$) as a function of temperature.

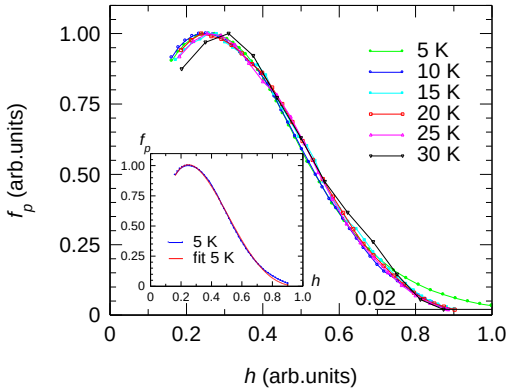

Fig. 11. Reduced pining force f_p vs. reduced magnetic field h at 5- 30 K. Inset presents the experimental and fitting curves of $f_p(h)$ at 5K.

When several mechanisms are simultaneously active with an equivalent weight, or, when their weight is temperature dependent, scaling procedure has limitations. For MgB_2 they are discussed in refs. [52, 53]. From the percolation theory considerations, Eisterer [54, 55] demonstrated that the position of the

pinning force peak (H_{peak}) depends also on the anisotropy factor (γ) and on the percolation threshold (p_c). Based on these results he indicated that the ratio $k_n = H_{peak} / H_n$, with H_n being the field at which the volume pinning force drops to half of its maximum, is expected to be 0.34 and 0.47 for the grain boundary pinning (GBP) and for the point pinning (PP), respectively. Nevertheless, k_n shows the pinning mechanism in the region of intermediate magnetic fields where H_{peak} and H_n are determined. The pinning-force-related parameters p, q, h_0 and k_n at different temperatures are shown in Figs. 12 - 14.

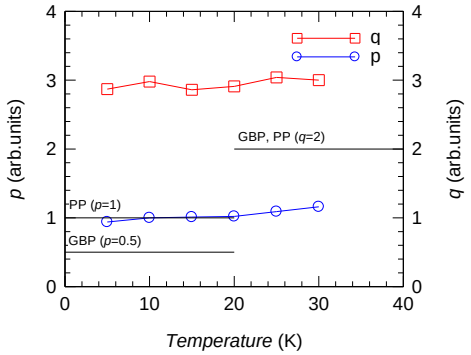

Fig. 12. Pinning-force-related parameters p and q vs. temperature.

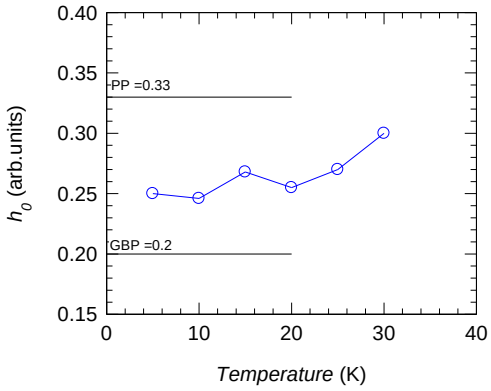

Fig. 13. Pinning-force-related parameter h_0 vs. temperature.

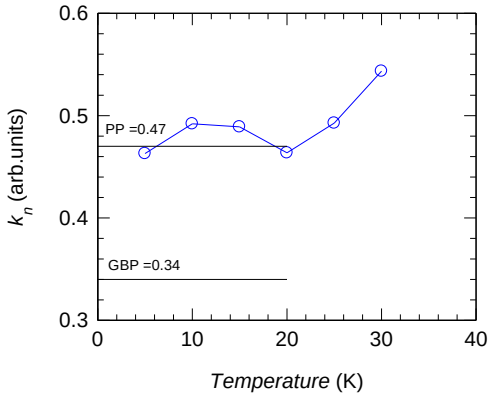

Fig. 14. Pinning-force-related parameter k_n vs. temperature.

Parameters k_n, h_0 and p suggest that the dominant pinning mechanism is of PP type. The GBP mechanism has a stronger contribution at lower temperatures. The parameter q takes values larger than theoretical ones (q = 2). The results for the MgB_2 core are similar to those for the bulk fabricated by SPS at 1150 °C [50].

6. Conclusions

In summary, powder-in-tube tapes of MgB_2 in Fe sheath were obtained by plastic deformation. Short specimens were processed by SPS at different temperatures. The optimum SPS temperature was 1050 °C. The core of this tape was electromagnetically characterized in detail. It was found that different characteristics of the MgB_2 core are similar to those of the bulk sample obtained by SPS at 1150 °C. This indicates that processes during spark plasma sintering of the bulk and of the tape's core develop in a similar manner. This enables SPS and, in the future, SPR as promising routes where the knowledge from bulks is transferable within a good approximation to tapes. However, in the case of tapes, one has to keep in mind the influence of the metal sheet on MgB_2 and of different aspects related to specifics of tapes processing. In this work a strong inter diffusion between Fe and MgB_2 damaged the tape's integrity when a high SPS temperature of 1150 °C was used. For processing at this high temperature search of other metal sheets is important and work in this direction is in progress. Pinning-force-related parameters indicate a major pinning contribution of PP type. The GBP pinning is stronger at low temperatures.

Acknowledgement

This work was performed within the Partnership Program in the Priority Domains – PN II funded by MEN-UEFISCDI, Project No 214/2014

BENZISUPRA. Authors also acknowledge Core Program PN16-480 P2, P3 and POC E-28, Romania.

R E F E R E N C E S

[1] *P.C. Canfield, D.K. Finnemore, S.L. Bud'ko, J.E. Ostenson, G. Lapertot, C.E. Cunningham and C. Petrovic*, "Superconductivity in Dense MgB_2 Wires", in Phys. Rev. Lett., **vol. 86**, 2001 pp. 2423-2426

[2] *C.E. Cunningham, C. Petrovic, G. Lapertot, S.L. Bud'ko, F. Laabs, W. Straszheim, D.K. Finnemore and P.C. Canfield*, "Synthesis and processing of MgB_2 powders and wires", in Physica C, **vol. 353**, 2001, pp 5-10

[3] *J.D. DeFouw and D.C. Dunand*, "In situ synthesis of superconducting MgB_2 fibers within a magnesium matrix", in Appl. Phys. Lett., **vol. 83**, 2003, pp. 120-122

[4] *K. Komori, K. Kawagishi, Y. Takano, H. Fujii, S. Arisawa, H. Kumakura, M. Fukutomi and K. Togano*, "Approach for the fabrication of MgB_2 superconducting tape with large in-field transport critical current density", in Appl. Phys. Lett., **vol. 81**, 2002, pp. 1047-1049

[5] *V. Ferrando, P. Orgiani, A. V. Pogrebnyakov, J. Chen, Qi Li, J. M. Redwing, and X. X. Xi*, "High upper critical field and irreversibility field in MgB_2 coated-conductor fibers", in Appl. Phys. Lett., **vol. 87**, 2005, 252509-3 pp.

[6] *M. Ranot, W.K. Seong, S.-G. Jung, W.N. Kang, J. Joo, C.-J. Kim, B.-H. Jun and S. Oh*, "Effect of SiC-Impurity Layer and Growth Temperature on MgB_2 Superconducting Tapes Fabricated by HPCVD", in Chem. Vapor Depos., **vol 18,** 2012, pp. 36-40

[7] *W.B.K. Putri, B. Kang, M. Ranot, J.H. Lee and W.N. Kang*, "A possibility of enhancing J_c in MgB_2 film grown on metallic hastelloy tape with the use of SiC buffer layer", in Prog. Supercond. Cryog., **vol. 16**, 2014, pp. 20-23

[8] *W.B.K. Putri, B. Kang, M. Ranot, J.H. Lee and W.N. Kang*, "Effect of Different Thickness Crystalline SiC-Buffer Layers on Superconducting Properties and Flux Pinning Mechanism of MgB_2 Films", in IEEE Trans. Magn., **vol 50**, 2014, 9000305-5pp.

[9] *R. Mahipal, S. Oh, K.C. Chung and W.N. Kang*, "MgB_2 coated conductors directly grown on flexible metallic Hastelloy tapes by hybrid physical–chemical vapor deposition", in Curr. Appl. Phys., **vol. 13**, 2013, pp. 1808-1812

[10] *H. Abe, K. Nishida, M. Imai, H. Kitazawa and K. Yoshii*, "Superconducting properties of MgB_2 films electroplated to stainless steel substrates", in Appl. Phys. Lett., **vol. 85**, 2004, pp. 6197-6199

[11] *H.L. Suo, C. Beneduce, M. Dhalle, N. Musolino, J.Y. Genoud and R. Flukiger*," Large transport critical currents in dense Fe- and Ni-clad MgB_2 superconducting tapes", in Appl. Phys. Lett., **vol. 79**, 2001, pp. 3116-3118

[12] *H. Kumakura, A. Matsumoto, H. Fujii and K. Togano*, "High transport critical current density obtained for powder-in-tube-processed MgB_2 tapes and wires using stainless steel and Cu–Ni tubes", in Appl. Phys. Lett., **vol. 79**, 2001, pp. 2435-2437

[13] *G. Grasso, A. Malagoli, C. Ferdeghini, S. Roncallo, V. Braccini, A.S. Siri and M.R. Cimberle*, "Large transport critical currents in unsintered MgB_2 superconducting tapes", in Appl. Phys. Lett., **vol 79**, 2001, pp. 230-232

[14] *A. Serquis, L. Civale, D.L. Hammon, J.Y. Coulter, X.Z. Liao, Y.T. Zhu, D.E. Peterson and F.M. Mueller*, "Microstructure and high critical current of powder-in-tube MgB_2", in Appl. Phys. Lett., **vol. 82**, 2003, pp. 1754-1756

[15] *H. Fang, S. Padmanabhan, Y.X. Zhou and K. Salama*, "High critical current density in iron-clad MgB_2 tapes", in Appl. Phys. Lett., **vol. 82**, 2003, pp. 4113-4115

[16] *H. Fang, P.T. Putman, S. Padmanabhan, Y.X. Zhou and K. Salama*," Transport critical current on Fe-sheathed MgB_2 coils", in Supercond. Sci. Technol., **vol. 17**, 2004, pp. 717-720

[17] *B.A. Glowacki, M. Majoros, M. Vickers, J.E. Evetts, Y. Shi and I. McDougall*, "Superconductivity of powder-in-tube MgB_2 wires", in Supercond. Sci. Technol., **vol. 14**, 2001, pp. 193-199

[18] *M.J. Tomsic*, "METHOD FOR MANUFACTURING MGB_2 INTERMETALLIC SUPERCONDUCTOR WIRES", in US Patent Specification, No 6687975, 2004

[19] *M.D. Sumption, M. Bhatia, X. Wu, M. Rindfleisch, M. Tomsic and E.W. Collings*, "Multifilamentary, in situ route, Cu-stabilized MgB_2 strands", in Supercond. Sci. Technol., **vol. 18**, 2005, pp. 730-734

[20] *P. Kováč, I. Hušek, L. Kopera, T. Melišek, A. Rosová and E. Dobročka*, "Properties of in situ made MgB_2 in Nb or Ti sheath", in Supercond. Sci. Technol., **vol. 26**, 2013, 025007-6 pp

[21] *C.E.J. Dancer, P. Mikheenko, A. Bevan, J.S. Abell, R.I. Todd and C.R.M. Grovenor*, "A study of the sintering behaviour of magnesium diboride", in J. Eur. Ceram. Soc., **vol. 29**, 2009, pp. 1817-1824

[22] *P. Lezza, R. Gladyshevskii, H.L. Suo and R. Flükiger*, "Quantitative study of the inhomogeneous distribution of phases in Fe-sheathed ex situ MgB_2 tapes", in Supercond. Sci. Technol., **vol. 18**, 2005, pp. 753-757

[23] *Y. Takano, H. Takeya, H. Fujii, H. Kumakura, T. Hatano, and K. Togano H. Kito and H. Ihara*, "Superconducting properties of MgB_2 bulk materials prepared by high-pressure sintering", in Appl. Phys. Lett., **vol. 78**, 2001, pp. 2914-2916

[24] *C.E.J. Dancer, D. Prabhakaran, M. Başoğlu, E. Yanmaz, H. Yan, M. Reece, R.I. Todd and C.R.M. Grovenor*, "Fabrication and properties of dense ex situ magnesium diboride bulk material synthesized using spark plasma sintering", in Supercond. Sci. Technol., vol. 22, 2009, 095003-7 pp.

[25] *S. Mizutani, A. Yamamoto, J.-I. Shimoyama, H. Ogino and K. Kishio*, "Understanding routes for high connectivity in ex situ MgB_2 by self-sintering", in Supercond. Sci. Technol., **vol. 27**, 2014, 044012-7 pp.

[26] *M.A. Susner, M. Bhatia, M.D. Sumption and E.W. Collings*, "Electrical resistivity, Debye temperature, and connectivity in heavily doped bulk MgB_2 superconductors", in J. Appl. Phys., **vol. 105**, 2009, 103916-3 pp.

[27] *J.M. Rowell*, "The widely variable resistivity of MgB_2 samples", in Supercond. Sci. Technol., **vol. 16**, 2003, pp. R17-27

[28] *T. Matsushita, M. Kiuchi, A. Yamamoto, A. Shimoyama and K. Kishio*, "Critical current density and flux pinning in superconducting MgB_2", in Physica C, **vol. 468**, 2008, pp. 1833-1835

[29] *M.A. Susner, T.W. Daniels, M.D. Sumption, M.A. Rindfleisch, C.J. Thong and E.W. Collings*, "Drawing induced texture and the evolution of superconductive properties with heat treatment time in powder-in-tube in situ processed MgB_2 strands", in Supercond. Sci. Technol., **vol. 25**, 2012, 065002-13 pp.

[30] *R. Flükiger, M.S.A. Hossain, C. Senatore, F. Buta and M. Rindfleisch*, "A New Generation of In Situ MgB_2 Wires With Improved J_c and B_{irr} Values Obtained by Cold Densification (CHPD)", in IEEE Trans. Appl. Supercond., **vol. 21**, 2011, pp. 2649-2654

[31] *R. Flükiger, M.S.A. Hossain, M. Kulich and C. Senatore*, "Technical Aspects of Cold High Pressure Densification (CHPD) on Long Lengths of *in situ* MgB_2 Wires With Enhanced J_c Values", in AIP Conf. Proc., **vol. 1435**, 2012, pp. 353-362

[32] *M.S.A. Hossain, A. Motaman, S. Barua, D. Patel, M. Mustapic, J.H. Kim, M. Maeda, M. Rindfleisch, M. Tomsic and O. Cicek*, "The roles of CHPD: superior critical current density

and n-value obtained in binary in situ MgB_2 cables", in Supercond. Sci. Technol., **vol. 27**, 2014, 095016-7 pp.

[33] *C. Zhou, P. Gao, H.J.G. Krooshoop, M. Dhallé, M.D. Sumption, M. Rindfleisch, M. Tomsic, M. Kulich, C. Senatore and A. Nijhuis*, "Intrawire resistance, AC loss and strain dependence of critical current in MgB_2 wires with and without cold high-pressure densification", in Supercond. Sci. Technol., **vol. 27**, 2014, 075002-5 pp.

[34] *W.J. Feng, S. Zhang, Y.Q. Guo, H. Yang, T.D. Xia, Z.Q. Wei*, "Fabrication of Ti doped MgB2/Cu superconducting wires by SHS method in an unsealed furnace", in Physica C, **vol. 470**, 2010, pp. 236-239

[35] *T. Cetner, A. Morawski, D. Gajda, W. Häßler, M. Rindfleisch, M. Tomsic, A. Zaleski, T. Czujko, E. Żuchowska and P. Przysłupski*, "Hot isostatic pressing of multifilamentary MgB2 wires in solid state media for large scale application", in Supercond. Sci. Technol., **vol. 28**, 2015, 045009-6 pp.

[36] *C.R.M. Grovenor, L. Goodsir, C.J. Salter, P. Kovac and I. Husek*, "Interfacial reactions and oxygen distribution in MgB_2 wires in Fe, stainless steel and Nb sheaths", in Supercond. Sci. Technol., **vol. 17**, 2004, pp. 479-484

[37] *J.-C. Grivel, R. Pinholt, N.H. Andersen, P. Kováč, I. Hušek and J. Homeyer*, "In situ investigations of phase transformations in Fe-sheathed MgB_2 wires", in Supercond. Sci. Technol., **vol. 19**, 2004, pp. 96-101

[38] *W.D. Kingery and M. Berg*, "Study of the Initial Stages of Sintering Solids by Viscous Flow, Evaporation-Condensation, and Self-Diffusion", in J. Appl. Phys., **vol. 26**, 2005, pp. 1205-1212

[39] *R.L. Coble*, "Sintering Crystalline Solids. I. Intermediate and Final State Diffusion Models", in J. Appl. Phys., **vol. 32**, 1961, pp. 787-792

[40] *R. Orru, R. Licheri, A.M. Locci, A. Cincotti, G. Cao*, "Consolidation/synthesis of materials by electric current activated/assisted sintering", in Mat. Sci. Engin. R, **vol. 63**, 2009, pp. 127–287

[41] *J.R. Groza, A. Zavaliangos*, "Sintering activation by external electrical field", in Mater. Sci. Eng. A, **vol. 287:2**, 2000, pp. 171–177

[42] *P. Badica, A. Crisan, G. Aldica, K. Endo, H. Borodianska, K. Togano, S. Awaji, K. Watanabe, Y. Sakka and O. Vasylkiv*, "'Beautiful' unconventional synthesis and processing technologies of superconductors and some other materials", in Sci. Technol. Adv. Mater., **vol. 12**, 2011, 013001-13 pp.

[43] *G. Aldica, D. Batalu, S. Popa, I. Ivan, P. Nita, Y. Sakka, O. Vasylkiv, L. Miu, I. Pasuk, P. Badica*, "Spark plasma sintering of MgB_2 in the two-temperature route", in Physica C, **vol. 477**, 2012, pp. 43-50

[44] *G. Aldica, M. Burdusel, S. Popa, M. Enculescu, I. Pasuk, P. Badica*, "The influence of heating rate on superconducting characteristics of MgB_2 obtained by spark plasma sintering technique", in Physica C, **vol. 519**, 2015, pp. 184-189

[45] *C.P. Bean*, "Magnetization of hard superconductors", in Phys. Rev. Lett., **vol. 8**, 1962, pp. 250-253

[46] *V.P.S. Awana, A. Vajpayee, M. Mudgel, V. Ganesan, A.M. Awasthi, G.L. Bhalla, H. Kishan*, "Physical property characterization of bulk MgB_2 superconductor", in The European Phys. J. B, **vol 62**, 2008, pp. 281–294

[47] *M. Takahashi, M. Koshimura and T. Abuzuka*, "Phase Diagram of Amorphous and Crystallized Fe-B Alloy System", in Jap. J. Appl. Phys., **vol. 20**, 1981, pp. 1821-1832

[48] *Z. Liu, Y. Zhong, D.G. Schlom, X.X. Xi and Q. Li*, "Computational thermodynamic modeling of the Mg–B system", in Calphad, **vol. 25**, 2001, pp. 299–303

[49] *F. Hayashi*, "Econometrics", in Princeton University Press, ISBN: 9780691010182, 0-691-01018-8, 2000, pp. 20

[50] *P. Badica, G. Aldica, A.M. Ionescu, M. Burdusel, D. Batalu*, "The influence of different additives on MgB_2 superconductor obtained by ex-situ Spark Plasma Sintering: pinning force aspects", Correlated Functional Oxides: Nanocomposites and Heterostructures, ed H Nishikawa et al, Springer, 2017, pp. 75-116.
[51] *D. Dew-Hughes*, "Flux pinning mechanisms in type II superconductors", in Philosophical Magazine, **vol. 30,** 1974, pp. 293-305
[52] *V. Sandu*, "Pinning-force scaling and its limitation in intermediate and high temperature superconductors", in Mod. Phys. Lett. B, **vol. 26**, 2012, 1230007-18 pp.
[53] *E. Martinez, P. Mikheenko, M. Martinez-Lopez, A. Millan, A. Bevan and J. S. Abell*, "Flux pinning force in bulk MgB_2 with variable grain size", in Phys. Rev. B, **vol. 75**, 2007, 134515-8 pp.
[54] *M. Eisterer*, "Magnetic properties and critical currents of MgB_2", in Supercond. Sci. Technol., **vol. 20**, 2007, pp R47-R73
[55] *M. Eisterer*, "Calculation of the volume pinning force in MgB_2 superconductors", in Phys. Rev. B, **vol. 77**, 2008, 144524-5 pp.